

Single - and double energy swift and slow heavy ion irradiated optical waveguides in Er: Tungstene-Tellurite glass and BGO for telecom applications

I. Bányász ^{a*}, J. Olivares ^{b,c}, O. Peña-Rodríguez ^{b,c}, Miguel L. Crespillo ^b, Z. Zolnai^d, M. Fried^d, T. Lohner^d, S. Berneschi ^{e,f}, G. Righini ^g, S. Pelli ^f, G. Nunzi Conti ^f

^a Department of Crystal Physics, Wigner Research Centre for Physics, Hungarian Academy of Sciences, P.O.B. 49, H-1525, Budapest, Hungary
^b Centro de Micro-Análisis de Materiales, Universidad Autónoma de Madrid (UAM), Cantoblanco, E-28049 Madrid, Spain
^c Instituto de Óptica, Consejo Superior de Investigaciones Científicas (CSIC), C/ Serrano 121, E-28006 Madrid, Spain
^d Research Institute for Technical Physics and Materials Science, Research Centre for Natural Sciences, Hungarian Academy of Sciences, Budapest, P.O.B. 49, H-1525 Hungary
^e “Enrico Fermi” Center for Study and Research, Piazza del Viminale 2, 00184 Roma, Italy
^f MDF-Lab, “Nello Carrara” Institute of Applied Physics, IFAC-CNR, Via Madonna del Piano 10, 50019
^gCorresponding author: banyasz.istvan@wigner.mta.hu

1

OUTLINE

1. Motivation
2. Design and fabrication of the waveguides
3. Spectroscopic ellipsometry
4. M-line spectroscopy
5. Conclusion and Outlook

2

1. Motivation

- Er³⁺- doped tungsten-tellurite glasses - very attractive materials for the fabrication of broadband amplifiers in wavelength division multiplexing (WDM) around 1.55 μm, as they exhibit large stimulated cross sections and broad emission bandwidth.
- Bi₄Ge₃O₁₂ (eulite type BGO) - well known scintillator material, also a rare-earth host material, photorefractive waveguides produced in it only using light ions in the past. Recently: MeV N⁺ ions and swift O⁵⁺ and C⁵⁺ ions, too*.
- Bi₁₂Ge₂₀ (sillenite type BGO) - high photoconductivity and photorefractive sensitivity in the visible and NIR – good candidate for real-time holography and optical phase conjugation, photorefractive waveguides produced in it only using light ions. No previous attempts of ion beam fabrication of waveguides in it.

*J. Yang, et al, Appl. Optics , 50, 6678 (2011)

3

2. Design and fabrication of the waveguides

2.1 SRIM calculations

2.1.1 Single- and double energy N⁺ ion irradiation in Er: Tungstene-Tellurite glass

Mechanism of waveguide formation : Reduced refr. index barrier layer around stopping range (dominant nuclear interaction)*

Implanted N⁺ distribution: SRIM 2012 code simulation

* I. Bányász, et al, IEEE Photonics Journal, 4, 721-7 (2012)

4

Fig. 1 Algebraic sum of the pairs of calculated N⁺ distributions along the sample depth.

Width of well and barrier vs. lower energy, two-energy N⁺ implanted Er: Te-glass. E₁ = 3.5 MeV

Fig. 2 Widths (at half maximum of the N⁺ distribution) of well and barrier layers vs. lower energy of N⁺ irradiation. Higher energy is kept constant at 3.5 MeV.

Irradiation conditions (at Wigner Research Centre, Budapest)
 Energy combinations: 3.5 MeV, 3.5 + 3.0 MeV and 3.5 + 2.5 MeV
 Total irradiation fluences: 10¹⁵ < F < 10¹⁷ ions/cm²

5

2.1.2 Single- and double-energy N⁺ ion irradiation in eulite (Bi₄Ge₃O₁₂) and sillenite (Bi₁₂Ge₂₀) type Bismuth Germanate crystals

Mechanism of waveguide formation : Reduced refr. index barrier layer around stopping range (dominant nuclear interaction) *.

Fig. 3 Double –energy N⁺ distributions along the sample depth in eulite (left) and sillenite (right) type BGO crystals.

*I. Bányász, et al, NIM-B, 286, 80–84 (2012).

6

Irradiation conditions (at Wigner Research Centre, Budapest)
 Energy combinations: 3.5 MeV, 3.5 + 3.25 MeV and 3.5 + 2.75 MeV
 Total irradiation fluences: $10^{15} < F < 10^{17}$ ions/cm²

2.1.3 Waveguide fabrication via irradiation of sillenite (Bi₁₂GeO₂₀) type Bismuth Germanate crystals with 25 MeV C⁵⁺ ions

Mechanism of waveguide formation : A reduced refr. index amorphous barrier layer is created around the maximum of the electronic stopping power, $S_e(z)$. Its thickness is controlled by the irradiated (low or ultralow) fluence (use of the electronic interaction)*.

Irradiation conditions (at CMAM, UAM, Madrid)
 Energy : 25 MeV
 Angles of incidence: 60° and 70°.
 Total irradiation fluences: $10^{13} < F < 10^{15}$ ions/cm²

*J. Olivares, et al, Appl. Phys. Lett., 86, 183501 (2005)

Fig. 4 SRIM calculation of $S_e(z)$ for 25 MeV C⁵⁺ with corrections for angle of incidence of 60° (left) and 70° (right) in sillenite type BGO crystal.

3. Spectroscopic ellipsometry
 Spectroscopic ellipsometer used: WOOLLAM M-2000DI.

Fig. 5 Measured and simulated ellipsometric spectra of a waveguide in an Er:Te glass, obtained with 1.5 MeV N⁺ ions at a fluence of 4×10^{16} ions/cm².

ψ = relative intensity change at reflection
 Δ = relative phase change at reflection

$\rho = tg \Psi e^{i\Delta}$

Optical model: 2-layer Cauchy dispersion

well
 barrier
 non irradiated bulk

SRIM

3.1 Results for Er:Te glass

Fig. 6 SRIM simulation and SE fit of the waveguide structure in Er:Te glass at various irradiation energies and fluences: **a)** E = 1.5 MeV, fluences are $1 \cdot 10^{16}$ and $4 \cdot 10^{16}$. **b)** E = 3.5 MeV, fluences are $1 \cdot 10^{16}$ and $8 \cdot 10^{16}$ ions/cm². **c)** E = 3.5 MeV + 3.0 MeV, fluence is $4 \cdot 10^{16}$ ions/cm².

3.2 Results for Eulytine and Sillenite type BGO

Fig. 7 SRIM simulation and SE fit of the waveguide structure in BGO and CaF₂ with 3.5 MeV N⁺ irradiation at various fluences: **a)** Eulytine, fluences are $0.2 \cdot 10^{16}$ and $1.6 \cdot 10^{16}$. **b)** Sillenite, fluences are $0.2 \cdot 10^{16}$ and $1.6 \cdot 10^{16}$ ions/cm².

4. M-line spectroscopy

COMPASSO, a semi-automatic m-line spectroscopic instrument, developed at IFAC, was used for the characterization of the planar waveguides implanted in the samples, except of the 25 MeV C⁵⁺ irradiated sillenite type BGO.

With COMPASSO, multi-wavelength m-line spectroscopy was performed at the following wavelengths:

635, 980, 1310 and 1550 nm.

Accuracy of the instrument is generally $\pm 1 \cdot 10^{-4}$ and $\pm 4 \cdot 10^{-4}$ on the effective refractive index and bulk refractive index, respectively. In the case of the N⁺-implanted planar waveguides in the Er:Te glass, due to the lower contrast in the measurement, the accuracy was lower, about $\pm 5 \cdot 10^{-4}$ and $\pm 1 \cdot 10^{-3}$ respectively. Due to the high refractive index of the bulk Er:Te glass (around 2.0 at 635 nm), and even higher of the sillenite BGO (about 2.55 at 635 nm) we used special rutile prisms to couple the light in the irradiated regions. **All the measurements presented here were performed in TE configuration.**

4.1 Results for Er:Te glass

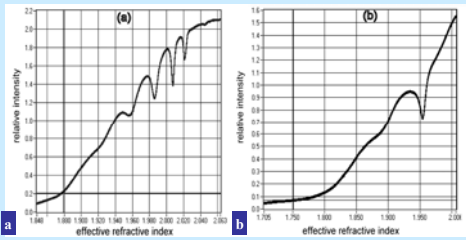


Fig. 8 M-line spectra of a waveguide in Er: Te glass. Fluence = $8 \cdot 10^{16}$ ions/cm², E = 3.5 MeV. (a) at 635 nm and (b) at 1550 nm.

13

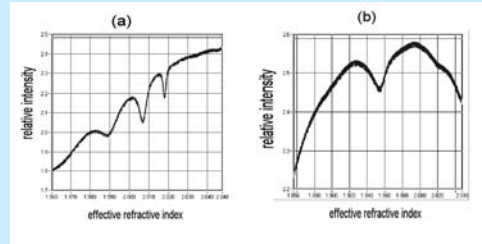


Fig. 9 M-line spectra of a waveguide in Er: Te glass, with double energy N⁺ ions at 3.5 MeV and 3.0 MeV, taken at 635 nm (a) and 1550 nm (b).

14

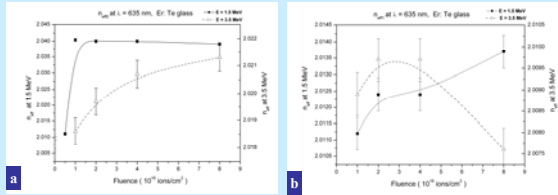


Fig. 10 Effective refractive indices of the a) fundamental and b) first modes vs. fluence at $\lambda = 635$ nm for 1.5 MeV N⁺ (full squares) and 3.5 MeV N⁺ (open triangles), Er: Te glass. Note the different abscissas for the two curves.

15

4.2 Results for Eulytine and Sillenite type BGO

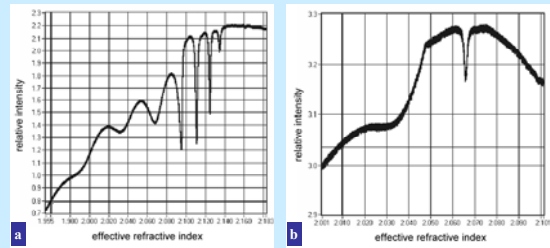


Fig. 11 M-line spectra of waveguide in Eulytine BGO. a) N⁺ Fluence = $1.6 \cdot 10^{16}$ ions/cm², E = 3.5 MeV, at 635 nm and b) at 1550 nm.

16

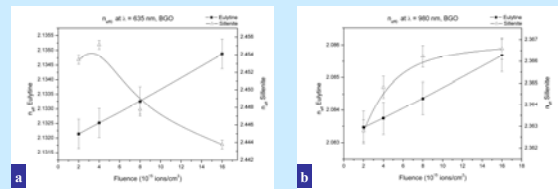


Fig. 12 Effective refractive indices at a) 635 nm and b) 980 nm of the fundamental mode vs. fluence for Eulytine (full squares) and Sillenite (open triangles) type BGO, irradiated with 3.5 MeV N⁺. Note the different abscissas for the two graphs.

17

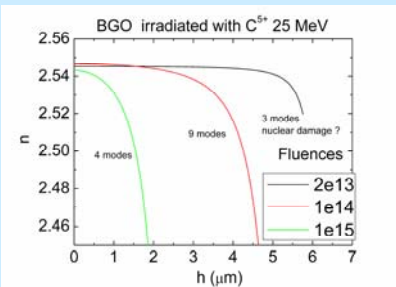


Fig. 13 Calculated refractive index profile of the waveguides in Sillenite type BGO irradiated with 25 MeV C⁵⁺ ions. Angle of incidence was 60°.

18

5. Conclusion and outlook

Working barrier-type slab waveguides in Er: tungsten-tellurite glass, and in Eulytine and Sillenite type BGO fabricated by 2.5 – 3.5 MeV N⁺ and 25 MeV C⁵⁺ ion irradiation, up to $\lambda = 1550$ nm.

Double-energy N⁺ ion irradiation in Er: tungsten-tellurite glass to suppress leaky modes and reduce propagation loss thanks to a thicker barrier layer.

A new method for waveguide characterization, making use of the multiwavelength m-line measurements has been developed (not discussed here) and is being improved by Dr. Stefano Pelli.

Propagation loss measurements in new single- and double N⁺ ion irradiated planar waveguides of increased lateral dimensions are under way.

Annealing experiments with all the available ion beam irradiated waveguides are under way. Refinement of spectroscopic ellipsometric model needed.

Special thanks to: Prof. M. Bettinelli and A. Speghini of the University of Verona for the Er:Te glass samples, to Mr. R. Calzolari of IFAC, Sesto Fiorentino and Mr. Gy. Matók of the Wigner research centre for polishing the glass and crystal samples.

This work has been supported by the Hungarian National Research Fund (OTKA-NKTH and OTKA) projects K 68688 and K 101223 and by a bilateral 2010-2012 CNR/MTA Italian – Hungarian project.

Thank you!

Preguntas

問題

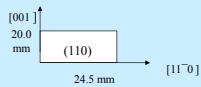
и замечания

The materials

Composition of the Er: tungsten - tellurite glass: 60 TeO₂ – 25 WO₃ – 15 Na₂O – 0.5 Er₂O₃ (mol%)

Bi₄Ge₃O₁₂ (eulytine type)
Thickness = 1 mm

Bi₁₂GeO₂₀ (sillenite type)
of the same orientation and thickness, but 14.0 mm x 21.5 mm.



Waveguide Characterization

The availability of data at several wavelengths (635, 980, 1310, and 1550 nm) has allowed us to obtain a more accurate and flexible data processing. Actually, assuming a Sellmeier-like law to account for chromatic dispersion for all layers, and using it in the fit process, it was possible to obtain the thickness of the guiding layer and the parameters A and B for the guiding and the barrier layers in a broad wavelength range.

$$n^2 = 1 + \frac{\lambda^2}{A\lambda^2 + B}$$

The fitting process allowed us to model through the A and B parameters the wavelength dependent refractive index of both the guiding (n_f) and barrier layers (n_s) by means of the A and B parameters and the above equation.

Moreover, the effective indices of the modes were calculated with the values of the numerical regression results and the same assumptions used in the fit process. The agreement between the experimental data (dots in Fig. 14) and the calculated effective indices is very good. Thickness of the guiding layer was assessed to be 2.2 μm, in agreement with SRIM simulations.

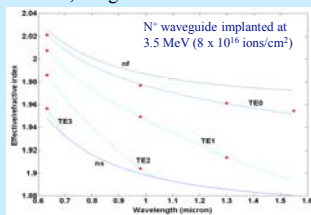


Fig. 14 Reconstruction of the refractive index of the guiding and barrier layers as a function of the wavelength. Sample irradiated with $8 \cdot 10^{16}$ ions/cm². Calculated effective indices of the modes are also shown.